Journal of Theoretical Biology 430 (2017) 103–108

Contents lists available at ScienceDirect

Journal of Theoretical Biology

journal homepage: www.elsevier.com/locate/jtbi

Modeling mechanical control of spindle orientation of intestinal crypt stem cells

Zsolt Bertalan[a,1], Stefano Zapperi[a,b,c,d,*], Caterina A.M. La Porta[e,*]

[a] Institute for Scientific Interchange Foundation, Via Chisola 5, 10126 Torino, Italy
[b] Center for Complexity and Biosystems, Department of Physics, University of Milan, via Celoria 16, 20133 Milano, Italy
[c] CNR - Consiglio Nazionale delle Ricerche, ICMATE, Via R. Cozzi 53, 20125 Milano, Italy
[d] Department of Applied Physics, Aalto University, P.O. Box 11100, FIN-00076 Aalto, Espoo, Finland
[e] Center for Complexity and Biosystems, Department of Environmental Science and Policy, University of Milan, via Celoria 26, 20133 Milano, Italy

ARTICLE INFO

Article history:
Received 5 May 2017
Revised 8 July 2017
Accepted 13 July 2017
Available online 15 July 2017

Keywords:
Spindle orientation
Symmetric and asymmetric cell division
Mechanics

ABSTRACT

Tissue development requires a control over the sequence of symmetric and asymmetric stem cell divisions to obtain the specific numbers of differentiated cells populating the tissue and stem cells residing in the niche. A good experimental model to study this process is the mouse intestinal crypt development, where it has been shown that stem cells follow an optimal strategy in which asymmetric division occurs only after all symmetric divisions have taken place to reach a fixed number of cells in the niche in the shortest time. Here we introduce a model of stem cell division that is able to explain the experimentally observed stem cell population dynamics by the effect of mechanical forces acting on the spindle. We also observe that the mechanically induced strategy for development is sub-optimal and crucially depends on the stiffness of the spindle. These findings highlight the crucial importance of mechanical forces for the development and maintenance of the intestinal crypt.

1. Introduction

Maintaining tissue homeostasis and regenerating damaged tissues both require an efficient control of cell divisions, a task that is accomplished by stem cells, a small group of cells residing in distinct niches within tissues. The niche is a confined space where a fixed number of stem cells and differentiated cells at different stages are present. One of the most studied and well known niches is the intestinal crypt where stem cells are located in invaginations of the epithelial layer providing protection from environmental dangers and facilitating signaling (Moore and Lemischka, 2006; Watt and Hogan, 2000). Stem cells have the capability to self-renew and to differentiate into more specialized progeny. This ability is realized by switching the mode of cell division from asymmetric, where one stem cell gives rise to another stem cell and a differentiated cell, to symmetric where one stem cell divides into two stem cells or possibly also into two differentiated cell. Asymmetric division is the dominant mechanism during tissue homeostasis since it enforces the conservation of the number of stem cells. Development and regeneration require instead symmetric stem cell divisions allowing the growth of the stem cell compartment (Lander et al., 2009).

The population dynamics of stem cells and differentiated cells has been investigated *in vivo* during the intestinal crypt morphogenesis (Itzkovitz et al., 2012). The results indicate that crypt development follows an optimal strategy, known as *bang-bang* control, in which stem cells first divide symmetrically, establishing a sufficiently large stem cell population, and only later switch to an asymmetric division mode that is needed to produce a mature crypt. Understanding the molecular factors controlling the transition from symmetric to asymmetric stem cell divisions has been the subject of intense research (Gruber et al., 2011; Lopez-Garcia et al., 2010; Morin and Bellaïche, 2011; Noatynska et al., 2012; Siller and Doe, 2009). It is generally believed that mechanical forces play an important regulatory role in cell division (for a recent review see Nestor-Bergmann et al., 2014). This general idea is related to the early observation by Hertwig that cells tend to divide along the long axis (the so-called Hertwig rule (Hertwig, 1884)) suggesting that cells are able to control their division mode according to their shape or their state of mechanical stress.

The orientation of the cell division process is mainly due to the action of the mitotic spindle: an dynamic structure consisting of

* Corresponding authors.
E-mail addresses: stefano.zapperi@unimi.it (S. Zapperi), caterina.laporta@unimi.it (C.A.M. La Porta).
[1] Present address: Braincon Technologies, Imagebiopsy Lab, Grinzinger Allee 5, 1190 Vienna, Austria

http://dx.doi.org/10.1016/j.jtbi.2017.07.012
0022-5193/

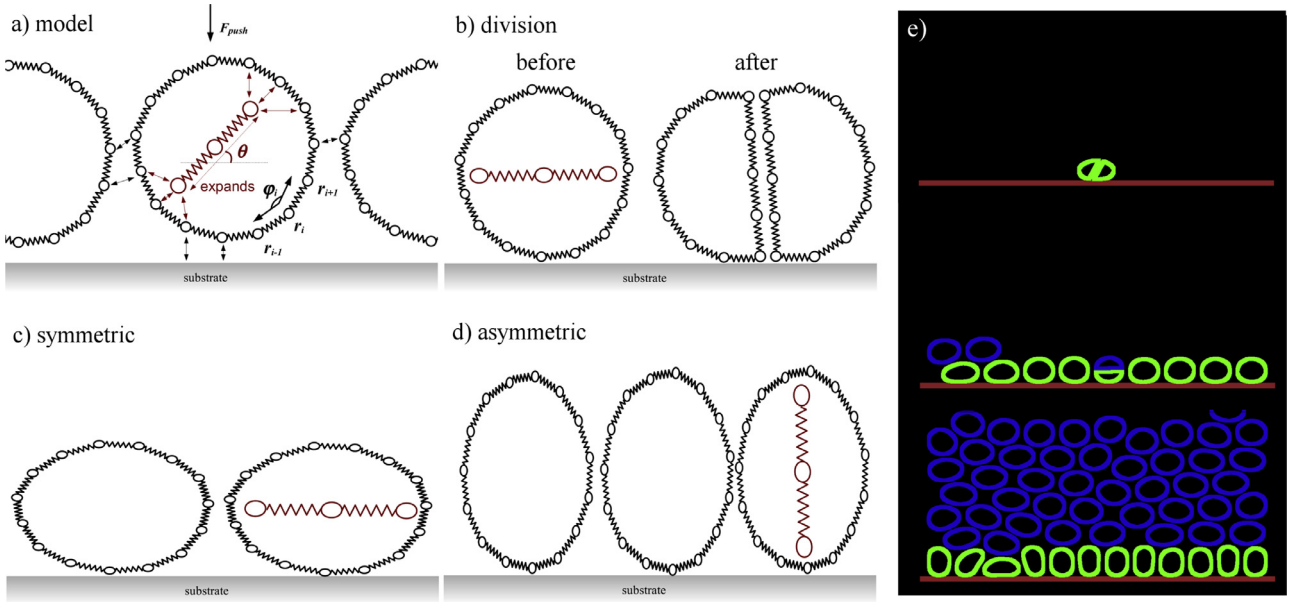

Fig. 1. a) Two-dimensional model of tissue generation. Cells are closed N-bead-spring-angle chains, while the spindle is an open 3-bead-spring-angle chain. All beads interact with every other bead and with a substrate by cut-off attractive LJ potentials. A downward force also acts on the top beads of the cells. When a cell divides, a spindle is inserted at a random angle. The rest length of the two segments of the spindle a_S are then elongated while the system is relaxed. Elongation is stopped when the elastic energy of the spindle reaches a critical value. The spindle orientation angle θ is measured with respect to the horizontal axis. b) The cell divides along an axis perpendicular to the spindle axis. The spindle is then removed and nodes and links are inserted into the two new cells accordingly. Two types of divisions may happen depending on the shape of the cells. c) Symmetric divisions, where $\theta < 45°$ happen in oblate cells while d) asymmetric divisions where $\theta > 45°$ take place in prolate cells. Only cells that are in contact with the substrate are allowed to divide. e) Illustration of tissue generation. Stem cells (green) divide first symmetrically (top panel) until a base layer of stem cells is formed. The base stem-cell layer then divides asymmetrically (middle panel) to form a tissue of differentiated cells (blue). The final equilbrium state is when a few layers of cells have been generated (bottom panel) and the base layer produces new differentiated cells on a regular basis, while the top layers of the tissue are ablated. (For interpretation of the references to colour in this figure legend, the reader is referred to the web version of this article.)

a large number of microtubules (MTs) growing from two centrosomes. The MTs in the spindle search and capture chromosomes, assemble them at the center of the cell and then separate them during anaphase (for review see Glotzer, 2009; Tanaka et al., 2010). Experiments in zebrafish (Campinho et al., 2013) and *Drosophila melanogaster* (Mao et al., 2013) provide direct evidence that spindle orientation during development is affected by stress patterns inside the tissue, so that spindles tend to orient along the axis of maximal tension (Campinho et al., 2013). The role of mechanical forces in determining the spindle orientation of dividing cells has also been investigated experimentally in human cell lines (Fink et al., 2011; Théry et al., 2007) and described in theoretical models (Jüschke et al., 2014; Pavin et al., 2012).

Here we propose a simple computational model illustrating how mechanical control of spindle orientation during tissue development naturally leads to a distinct sequence of symmetric and asymmetric divisions that is in close agreement with experimental results (Itzkovitz et al., 2012). Our results suggest that the *bang-bang* control strategy observed in intestinal crypt morphogenesis is a result of mechanical forces.

2. Model

We consider a two-dimensional model of cell division in which cells divide according to the spindle direction, as illustrated in Fig. 1. Cells are modeled as closed bead-spring-angle chains with N segments, and the rest angle between segments φ_0 is chosen so that unconstrained, the cell takes the shape of a regular polygon with M nodes. Accordingly, the radius of a cell is approximately $R \approx Ma/2\pi$, where a is the rest length between chain segments. Similarly, the spindle is described by a segment discretized by two elastic springs, whose rest length is slowly increased during cell division. The internal energy of the discretized elastic lines describing the cell boundary and the spindle are given by

$$\mathcal{E}_{el} = \sum_i \frac{1}{2} k_X (|\mathbf{r}_{i+1} - \mathbf{r}_i| - a)^2 - \frac{B_X}{a} \cos(\varphi_i - \varphi_0), \tag{1}$$

where k_X and B_X are the spring and bending stiffness constants, respectively. When we have to refer to these constants we will use the subscript X = C for the cell boundary and the subscript X = S for the spindle.

All beads in the system interact with each other, and cell beads also interact with a substrate via Lennard–Jones (LJ) potentials with a cut-off, given by

$$V_{LJ}(r) = 4\epsilon \left[\left(\frac{\sigma}{r}\right)^{12} - \left(\frac{\sigma}{r}\right)^{6} \right] \quad r < r_C. \tag{2}$$

Each interaction, cell-cell, cell-spindle and cell-substrate, has its own set of LJ parameters, ϵ, σ and r_c. The LJ parameters are chosen so that the potentials are slightly attractive, $r_C \gtrsim \sigma = a_C$. The system is evolved by solving overdamped Newton equations (no temperature), $\dot{\mathbf{r}} = dV/d\mathbf{r}$ for each bead. In our simulations we use $M = 20$ nodes per cell, so that $\varphi = 2\pi/n$. The length scale is set to $a = 5$ μm and the energy scale to $e = 10^{-15}$ J. All other units are derived from these two measures. The list of all parameters employed is reported in Table 1.

The tissue is generated by a set of cell divisions, starting from a single cell. A fixed force F_{push} in the direction of the substrate acts on the top cell-nodes. If the vertical direction is y, the top nodes of the cells are those for which $y_i > \Sigma_j y_j/M$, where i, j are bead indexes and the sum is over the beads in a cell boundary. During each step of tissue growth, we randomly chose a cell in contact with the substrate, and the spindle is slowly extended. When the elastic spindle energy reaches the critical value $0.15 k_S a_S$ due to compression by the cell walls its growth stops and the cell divides. This critical value is chosen small enough so that the spindle does

Table 1
List of parameters used in simulations.

Parameter	Symbol	Value	Note
LJ cutoff	r_c	$2.5a$	$a = 5$ μm
LJ sigma	σ	$2.1a$	
cell-cell adhesion	ϵ_{cc}	$1.5e$	$e = 10^{-15}$ J, per node (Simson et al., 1998)
cell-spindle adhesion	ϵ_{sc}	$1.1e$	
cell radius	R	$3.0a$	
static force	f_p	$3.0p$	$p = 2 \cdot 10^{-8}$ N; small, hypothetical ECM bias
simulation box size	x_f	11	undeformed cells
spindle bending stiffness	B_S	$150b$	$b = 10^{-20}$ Nm^2, estimate for model, spindles do not bend
spindle stiffness	k	0.01–10 s	$s = 10^{-9}$ N/m, estimate
cortex bending stiffness	B_C	$15b$	corresponds to cell Youngs modulus of 100 Pa (Kamgoué et al., 2007)
cortex extension stiffness	k_C	$100b$	

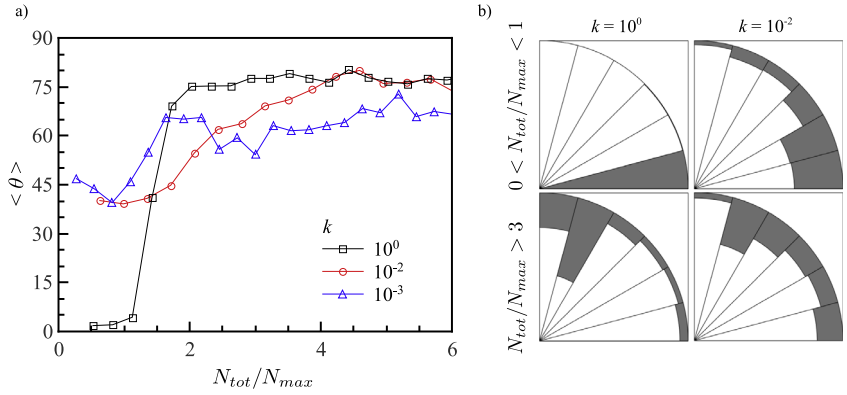

Fig. 2. a) Average spindle-angle orientation as a function of cell density, i.e. the total number of cells N_{tot} divided by the $N_{\max}$, the number of undeformed cells that would fit in the simulation box. The average spindle orientation angle $\langle\theta\rangle$ is plotted as a function of $N_{tot}/N_{\max}$, for different spindle stiffness k. A small angle indicates symmetric division while a large angle corresponds to asymmetric divisions. When the spindle is rigid there is a marked separation between symmetric and asymmetric division phases. b) Angle distributions at various densities related to panel a). Angle distributions depend on time and cross over from a symmetric dominated phase (for $N_{tot}/N_{\max} < 1$) to a more asymmetric phase (for $N_{tot}/N_{\max} > 3$), but the transition is sharper for rigid spindles.

not distort the cell shape. This procedure spontaneously leads to an alignment of the spindle axis along the direction offering minimal mechanical resistance. The spindle bending stiffness is sufficiently large that in practice the spindle beads are always straight, allowing for the measurement of a clearly defined orientation angle θ. Cell division is modeled simply by splitting the dividing cell along the axis of the spindle which is then removed. Half of the beads go into the new cell, half of the beads stay in the old cell, while new beads are added and linked up to form two new cells as shown in Fig. 1b).

The base layer is generated by symmetric division – we call a division symmetric, if $\theta < 45°$ and the cell is in contact with the substrate. The base cell layer fills up and its expansion is constricted by imposed hard walls which interact with cells by LJ potentials with the parameters of the cell-cell interaction. The geometry we adopt is a simplified version of the actual stem cell niche, but retains the important character of being strongly confined. This constriction and filling up squeezes the basal cells until they become prolate in shape, and the spindle of a dividing cell will spontaneously orient horizontally $\theta > 45°$, leading to what we define as an asymmetric division. Cells that have been generated by asymmetric division are no longer able to divide and make up the (differentiated) tissue. This procedure is illustrated in Fig. 1c, where the differentiated cells are colored blue, while the stem cells are shown in green.

The distinction between symmetric and asymmetric divisions adopted in the present model is motivated by experimental observations suggesting that stem cells differentiate when they loose contact with the base of their niche (Knoblich, 2008). Hence, when the division plane is parallel to the substrate one of the two daughter cells looses contact with it and differentiates while the other cell retains its stem character. Conversely, when the division plane is perpendicular to the substrate both daughter cells remain in contact with the substrate and do not differentiate. A similar relation between the spindle axis and the symmetric or asymmetric nature of the division was established *in vivo* in mice neural stem cells (Gruber et al., 2011).

3. Results

3.1. Simulations of tissue development

If we consider a confined base layer of length L, we can fit in it $N_{\max} = L/2R$ cells of radius R without causing any cell deformation. Since cells are deformable, however, there will be more than $N_{\max}$ cells in the base layer. The cell density is simply defined as $\rho = N/N_0$ where N is the number of cells in the system. Only for $N_{tot}/N_{\max} > 1$ there are enough cell to fill the base layer, and further symmetric divisions produce compression in the system. Hence we can expect that the transition between symmetric and asymmetric cell division should take place for $N_{tot}/N_{\max} > 1$. Fig. 2a shows indeed the evolution of the division angle θ as a function of the number of cells in the system. For all values of the spindle stiffness we observe an increase of θ with $N_{tot}/N_{\max}$ indicating a transition from symmetric to asymmetric cell divisions. The precise location of the transition point depends on the elastic properties of the cells and for stiff spindles ($k = 1$) it is at $N_{tot}/N_{\max} \approx 1.5$. For softer spindles ($k \leq 10^{-2}$), however, the transition is less sharp and the division angle increases smoothly.

Angle distribution histograms corresponding to the averages shown in Fig. 2a are shown in Fig. 2b, where spindle angles have been binned into 15°-wide segments. At low densities

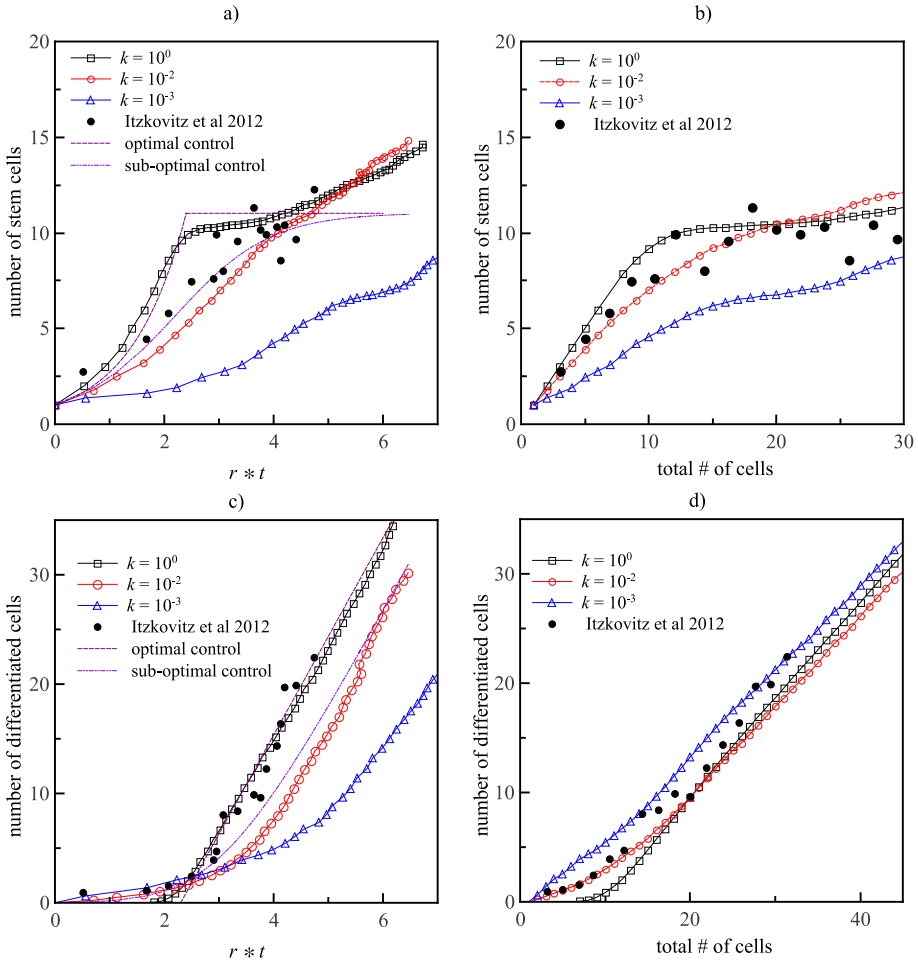

Fig. 3. a) The number of stem cells as a function of time rescaled to the division rate r. The plots show the averages over 100 samples. While for the rigid spindle case it is evident that a transition takes place between symmetric (stem cell generation) and asymmetric divisions as the base layer is formed, the transition is less sharp for floppy spindles. We also report experimental data from Ref. Itzkovitz et al. (2012) and fits from optimal and sub-optimal control theory. b) Same data as in a) but plotted in terms of the number of divisions. c) The number of differentiated cells for the same cases as reported in a) as a function of the rescaled time. d) Same data as in c) but plotted as a function of the number of divisions.

$N_{tot}/N_{\max} < 1$, the distribution for stiff spindles is such that all angles are lower than 15°, while for softer spindles the distribution is much broader. At high densities, the distribution broadens considerably in the case of the stiff spindle while for the softer spindle the distribution remains broad, but the peak shifts from symmetric to asymmetric divisions.

To make the symmetric/asymmetric transition clearer and to relate to previous experimental results (Itzkovitz et al., 2012), we plot the number of stem cells (Fig. 3a) and differentiated cells (Fig. 3c) versus time or equivalently the total number of cells as the tissue generates (Fig. 3b and d, respectively). The results clearly show that first the stem cells are generated by symmetric divisions and then the rest of the tissue is generated by asymmetric divisions from the stem cells in a way that closely follows the experimental results of Ref. Itzkovitz et al. (2012), see also Fig. 4.

3.2. Relations with control theory

The results reported in Fig. 3 compare very nicely with the *bang-bang* solution of optimal control theory (Itzkovitz et al., 2012). In this theory, one searches for an optimal solution of the problem under given constraints. In our case, we start from n_0 stem cells and N_0 differentiated cells, impose the dynamic equations

$$\dot{n} = rp(t)n(t)$$

$$\dot{N} = r(1 - p(t))n(t),$$

where r is the division rate of the stem cells, and search for the optimal solution to $p(t)$, the probability to divide symmetrically at time t, to reach a prescribed final configuration (n_T, N_T) in the shortest time. An additional constraint is provided by the space available for stem cells, since the cells do not divide when they are

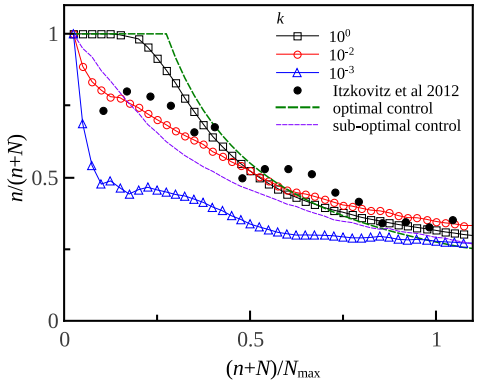

Fig. 4. The fraction of stem cells as a function of the (normalized) total number of cells for simulations with different spindle stiffness k and for experiments from Ref. Itzkovitz et al. (2012). The results of optimal control theory is also reported.

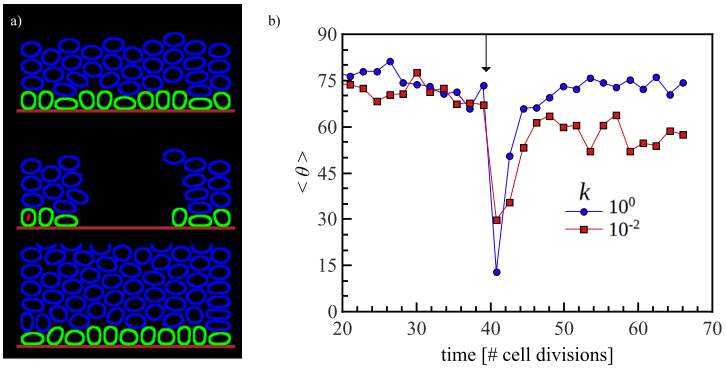

Fig. 5. Simulations of wound healing. a) We let the system relax and let the tissue generate (top), then we delete cells in a block of half the width of the simulation box (middle) and then let the wound close (bottom). b) Healing properties of the tissue expressed as the mean spindle-orientation angle versus time, the cut is indicated by the arrow. For rigid spindles, the tissue regenerates by first rebuilding the base layer with symmetric divisions and then regenerating the rest of the tissue with asymmetric divisions. On the other hand, in the floppy case the wound closes, but $\langle\theta\rangle$ does not reach the equilibrium level.

not in contact with the base layer. This constraint ideally caps the maximum number of stem cells at $n_{\max}$. Since the cells are elastic objects, however, the introduction of a hard cutoff is does not rigorously apply, although it simplifies considerably the model.

The solution to the problem is well known (see Itzkovitz et al., 2012 and references therein), and is simply given by $p(t) = 1-\theta(t-t_f)$, a step function, also called the *bang-bang* solution (Itzkovitz et al., 2012). In practice, the *bang-bang* solution means that first all stem cells are generated, and then the cells differentiate to generate the tissue. Here, $t_f = \ln(n_{\max}/n_0)/r$ is the time needed to reach the maximum number of stem cells. The solutions to the dynamic equations become simply

$$n(t) = n_0 \exp\left[r\min(t,t_f)\right]$$
$$N(t) = N_0 + t\theta(t-t_f)n_0\exp(rt_f),$$

plotted in Fig. 3a and c.

We can see that the optimal solution compares well with experiments and simulations of the rigid spindle case for the number of differentiated cells but overestimates the number of stem cells. We therefore consider sub-optimal solutions to the problem which would deviate from the sharp step function for $p(t)$, and could describe better the data. Here, we suppose that $p(t)$ deviates from the sharp step-function and set $p(t) = 1-(\tanh((t-t_f)/\tau)+1)/2$, so that the solutions to the dynamical equations are then

$$n_{so}(t) = n_0\exp(rt/2)\left[\frac{\cosh((t-t_f)/\tau)}{\cosh(t_f/\tau)}\right]^{-\tau/2}$$
$$N_{so}(t) = N_0 + r\int_0^t n_{so}(t')dt' - (n_{so}(t)-n_{so}(0))$$
$$\approx N_0 + tn_{\max} \quad \text{for} \quad t \gg t_f,$$

where the subscript *so* indicates sub-optimal. The time f loses in this case its interpretation as the time to reach the maximum number of stem cells, because of the absence of clear cut-offs and has to be determined numerically from the dynamic equations together with τ, to have $n(t\to\infty)\approx n_{\max}$. Sub-optimal solutions are also drawn in Fig. 3a and c where we see that they describe better the evolution of the number of stem cells and are in close agreement with the result for softer spindles.

For our simulations we have chosen $(n_0, N_0) = (1,0)$, $n_{\max} = n_T = 11$ and $N_T = 40$, so that approximately four layers of differentiated cells are generated, and we have set, without loss of generality, the division rate to unity $r = 1$. The optimal solution yields $t_f = \ln(11) \approx 2.4$. For the sub-optimal solution that best fits the data for $k = 10^{-2}$, we get $\tau \approx 1.7$ and $t_f \approx 2.4$. The results show that the sub-optimal case reaches only $N \approx 32$ differentiated cells in the time it takes for the optimal case to reach $N \approx 40$ cells. If the tissue/generation were to stop at fixed times T, the tissue generated by cells with softer spindles would be only 0.8 times the size of a corresponding tissue with rigid spindles.

3.3. Wound healing

Our mechanical model for spindle orientation can also be used to investigate wound healing. To this end, we simulate the model until we reach a tissue with four layer and then suddenly remove the cells in a block of half the width of the simulation box. We then observe the wound closure process and monitor the division angle of the stem cells as a function of time. Fig. 5 shows that stem cells respond to wound by triggering symmetric division and then rapidly restoring the damaged tissue through asymmetric cell divisions. When the spindle is softer the recovery is slower than in the case of a stiff spindle.

4. Conclusions

In this paper, we have proposed a mechanical model of spindle orientation during stem cell division. In the model the axis of division is set by the spindle, whose orientation reflect the integration of mechanical forces acting on the cell. We have used the model to simulate the development of a layered tissue, focusing on the crossover from symmetric to asymmetric stem cell divisions. Our model shows that mechanical constraints impose a definite pattern of stem cell division where initially stem cells always divide symmetrically until the base layer of the tissue is filled completely. At this point further symmetric divisions are hindered due to the horizontal compression of the layer leading to a reorientation of spindle axis along the vertical direction. Hence, the mode of division switches to an asymmetric one, with one stem cell remaining in the base layer and one differentiated cell populating the upper layers of the tissue. The precise form of the crossover is found to depend on the stiffness of the spindle: for stiff spindles the crossover between symmetric and asymmetric division is sharp while it is smoother for softer spindles.

We compare our simulation results with experimental results on mice intestinal crypt development (Itzkovitz et al., 2012) and find very good agreement. The experimental results were previously interpreted in terms of control theory, according to which a switch between symmetric and asymmetric division would be an optimal strategy for development. Here we suggest that such a control involves mechanical constraints. Furthermore, we show that experimental and numerical results are more compatible with

a sub-optimal strategy than with an optimal one. An optimal strategy would arise only in the limit of extremely stiff spindles but experiment results are closer to simulations of softer spindles. Finally, we use the model to simulate the process of wound healing and find that the process occurs faster for stiffer spindles. All together our results explain how the niche is able to maintain a fixed number of stem cells using also a simple mechanical control mechanism linked to the spindle orientation. Our simple model can be generalized to include more complex conditions but already captures the key ingredients of the process.

Acknowledgments

ZB and SZ are supported by the ERC Advanced Grant SIZEFFECTS. SZ acknowledges support from the Academy of Finland FiDiPro progam, project 13282993.

References

Campinho, P., Behrndt, M., Ranft, J., Risler, T., Minc, N., Heisenberg, C.-P., 2013. Tension-oriented cell divisions limit anisotropic tissue tension in epithelial spreading during zebrafish epiboly. Nat. Cell Biol. 15 (12), 1405–1414. doi:10.1038/ncb2869.

Fink, J., Carpi, N., Betz, T., Bétard, A., Chebah, M., Azioune, A., Bornens, M., Sykes, C., Fetler, L., Cuvelier, D., Piel, M., 2011. External forces control mitotic spindle positioning. Nat. Cell Biol. 13 (7), 771–778. doi:10.1038/ncb2269.

Glotzer, M., 2009. The 3ms of central spindle assembly: microtubules, motors and maps. Nat. Rev. Mol. Cell Biol. 10 (1), 9–20. doi:10.1038/nrm2609.

Gruber, R., Zhou, Z., Sukchev, M., Joerss, T., Frappart, P.-O., Wang, Z.-Q., 2011. Mcph1 regulates the neuroprogenitor division mode by coupling the centrosomal cycle with mitotic entry through the chk1-cdc25 pathway. Nat. Cell Biol. 13 (11), 1325–1334. doi:10.1038/ncb2342.

Hertwig, R., 1884. Erythropsis agilis, eine neue protozoe. gegenbaurs morphologisches jahrbuch. Zeitschrift für Anatomie und Entwicklungsgeschichte 10, 204–212.

Itzkovitz, S., Blat, I.C., Jacks, T., Clevers, H., van Oudenaarden, A., 2012. Optimality in the development of intestinal crypts. Cell 148 (3), 608–619. doi:10.1016/j.cell.2011.12.025.

Jüschke, C., Xie, Y., Postiglione, M.P., Knoblich, J.A., 2014. Analysis and modeling of mitotic spindle orientations in three dimensions. Proc. Natl. Acad. Sci. 111 (3), 1014–1019.

Kamgoué, A., Ohayon, J., Tracqui, P., 2007. Estimation of cell young's modulus of adherent cells probed by optical and magnetic tweezers: influence of cell thickness and bead immersion. J. Biomech. Eng. 129 (4), 523–530.

Knoblich, J.A., 2008. Mechanisms of asymmetric stem cell division. Cell 132 (4), 583–597.

Lander, A.D., Gokoffski, K.K., Wan, F.Y.M., Nie, Q., Calof, A.L., 2009. Cell lineages and the logic of proliferative control. PLoS Biol. 7 (1), e15. doi:10.1371/journal.pbio.1000015.

Lopez-Garcia, C., Klein, A.M., Simons, B.D., Winton, D.J., 2010. Intestinal stem cell replacement follows a pattern of neutral drift. Science 330 (6005), 822–825. doi:10.1126/science.1196236.

Mao, Y., Tournier, A.L., Hoppe, A., Kester, L., Thompson, B.J., Tapon, N., 2013. Differential proliferation rates generate patterns of mechanical tension that orient tissue growth. EMBO J. 32 (21), 2790–2803. doi:10.1038/emboj.2013.197.

Moore, K.A., Lemischka, I.R., 2006. Stem cells and their niches. Science 311 (5769), 1880–1885. doi:10.1126/science.1110542.

Morin, X., Bellaïche, Y., 2011. Mitotic spindle orientation in asymmetric and symmetric cell divisions during animal development. Dev. Cell. 21 (1), 102–119. doi:10.1016/j.devcel.2011.06.012.

Nestor-Bergmann, A., Goddard, G., Woolner, S., 2014. Force and the spindle: Mechanical cues in mitotic spindle orientation. In: Seminars in cell & developmental biology, Vol. 34. Elsevier, pp. 133–139.

Noatynska, A., Gotta, M., Meraldi, P., 2012. Mitotic spindle (dis)orientation and disease: cause or consequence? J. Cell Biol. 199 (7), 1025–1035. doi:10.1083/jcb.201209015.

Pavin, N., Laan, L., Ma, R., Dogterom, M., Jülicher, F., 2012. Positioning of microtubule organizing centers by cortical pushing and pulling forces. New J. Phys. 14 (10), 105025.

Siller, K.H., Doe, C.Q., 2009. Spindle orientation during asymmetric cell division. Nat. Cell Biol. 11 (4), 365–374. doi:10.1038/ncb0409-365.

Simson, R., Wallraff, E., Faix, J., Niewöhner, J., Gerisch, G., Sackmann, E., 1998. Membrane bending modulus and adhesion energy of wild-type and mutant cells of dictyostelium lacking talin or cortexillins. Biophys. J. 74 (1), 514–522.

Tanaka, K., Kitamura, E., Tanaka, T.U., 2010. Live-cell analysis of kinetochore-microtubule interaction in budding yeast. Methods 51 (2), 206–213. doi:10.1016/j.ymeth.2010.01.017.

Théry, M., Jiménez-Dalmaroni, A., Racine, V., Bornens, M., Jülicher, F., 2007. Experimental and theoretical study of mitotic spindle orientation. Nature 447 (7143), 493–496.

Watt, F.M., Hogan, B.L., 2000. Out of eden: stem cells and their niches. Science 287 (5457), 1427–1430.